

Corrosion inhibition of aluminum by novel phthalocyanines in hydrochloric acid solution

O. K. Özdemir · A. Aytaç · D. Atilla ·
M. Durmuş

Received: 28 February 2010/Accepted: 27 July 2010/Published online: 5 October 2010
© Springer Science+Business Media, LLC 2010

Abstract The corrosion inhibition characteristics of quaternized 1,(4)-tetrakis[(2-mercaptop)pyridine]phthalocyanine (**I**) and 2,3-octakis[(2-mercaptop)pyridine] phthalocyanine (**II**) on aluminum in 0.1 M HCl solution has been studied by means of potentiodynamic polarization and electrochemical impedance spectroscopy (EIS) techniques. The maximum inhibition efficiency was obtained for compound **I** with two-electrochemical techniques applied. Langmuir isotherm fits well the experimental data. The inhibition efficiency increases with increase in the phthalocyanine concentration, but decreases with an increase in temperature. The phthalocyanines act predominately as cathodic inhibitor.

Introduction

The resistance of aluminum against corrosion in aqueous media can be attributed to a rapidly formed surface oxide film. Therefore, aluminum has been known to exhibit very different electrochemical properties in different aqueous electrolytes. While certain anions are essential in obtaining anodic oxide films with porous or non-porous structure, other aggressive anions like chloride creates extensive

localized attack. Generally, localized corrosion can be prevented by the action of adsorptive inhibitors, which prevent the adsorption of the aggressive anions, or by the formation of a more resistant oxide film on the metal surface. In the last few years, there has been increasing interest in macrocyclic compounds as corrosion inhibitors in acidic environments [1–11].

Phthalocyanines exhibit several interesting properties and applications due to their highly delocalized conjugated π electron system. The high inhibition action of the phthalocyanines is attributable to their strong chemical adsorption on the metal surface, which is determined by planarity and lone pairs of electrons in heteroatoms [12, 13]. Since the 1980s, there have been studies on the performance of phthalocyanines and porphyrins [14].

The main objective of the present work is to investigate the influence of the novel 1,(4)-tetrakis[(2-mercaptop)pyridine]phthalocyanine (**I**) and quaternized Octakis[(2-mercaptop) pyridine]phthalocyanine (**II**) as an inhibitor for acid corrosion of aluminum. The study employed potentiodynamic and electrochemical impedance technique.

Experimental

Inhibitor compounds

3-Nitrophthalonitrile, 4-nitrophthalonitrile, 4,5-dichlorophthalonitrile, 4-(2-mercaptop-pyridine)phthalonitrile and 3-(2-mercaptop-pyridine)phthalonitrile were synthesized and purified according to literature [15–17].

Quaternized 2,(3)-tetrakis[(2-mercaptop)pyridine]phthalocyanine was prepared according to the method previously reported by Smith et al. [18]. 2,(3)-Tetrakis[(2-mercaptop)-pyridine]phthalocyanine (168 mg, 0.177 mmol) was heated

O. K. Özdemir · A. Aytaç
Department of Materials Science and Engineering, Gebze
Institute of Technology, 41400 Gebze, Kocaeli, Turkey

A. Aytaç (✉)
Department of Chemistry, Faculty of Science, Gazi University,
Teknikokullar, 06500 Ankara, Turkey
e-mail: aytaca@gazi.edu.tr; aaytac@gyte.edu.tr

D. Atilla · M. Durmuş
Department of Chemistry, Gebze Institute of Technology,
41400 Gebze, Kocaeli, Turkey

to 120 °C in freshly distilled dimethylformamide (5 mL) and dimethyl sulfate (0.168 mL) was added dropwise. The mixture was stirred at 120 °C for 12 h. After this time, the mixture was cooled to room temperature and the product was precipitated with hot acetone and collected by filtration. The green solid product was washed successively with hot ethyl acetate, chloroform, *n*-hexane, CCl₄, and diethylether. The resulting hygroscopic product was dried over phosphorous pentoxide. Quaternized 1,(4)-tetrakis[(2-mercaptop)pyridine]phthalocyanine (**I**) and quaternized 2,3-octakis[(2-mercaptop)pyridine]phthalocyanine (**II**) was synthesized according to same procedure used for compound quaternized 2,(3)-tetrakis[(2-mercaptop)pyridine]phthalocyanine.

The molecule structure and short name of used phthalocyanines are shown in Table 1.

Preparation of specimens

The sample selected for the study was 99.998% pure aluminum. Specimens used in the electrochemical measurement were mechanically cut into coupons of dimension 1 cm × 1 cm. Before each experiment, the electrodes were polished with a sequence of emery papers of different grades. Then they were degreased in distilled water and ethanol, dried in acetone. The working electrode was

inserted in sample holder so that its polished surface area (1.00 cm²) was in contact with the solution.

The solutions used for electrochemical test were prepared by 0.1 M HCl with addition of the phthalocyanine compounds that concentrations varied from 1.0×10^{-6} to 1.0×10^{-3} M. All chemicals purchased were of analytical reagent grade and were used without further purification.

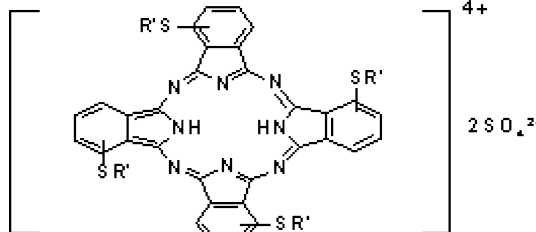
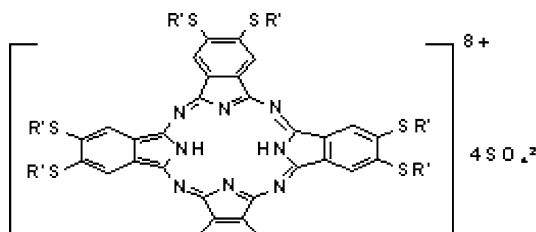
Electrochemical measurement

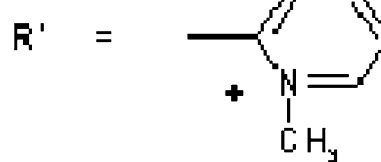
Electrochemical impedance spectroscopy (EIS) measurements and potentiodynamic polarization studies were carried out using VoltaLab 80 Radiometer potentiostat. Electrochemical experiments were performed in a conventional three electrodes electrochemical cell at 25 °C with a platinum counter electrode and Ag/AgCl reference electrode with a Lugin capillary.

The EIS measurements were conducted after 30 min immersion in experimental solution that ensured a system in equilibrium. The frequency range was 100 kHz to 20 mHz at OCP. The EIS data are presented in the form of Nyquist diagrams.

The potentiodynamic polarization curves were obtained with a scan rate of 1 mV/s in the potential range from −950 to −650 mV relative to the corrosion potential.

Table 1 Molecular structures and short names of phthalocyanines

Inhibitor name (short name)	Molecule structure
1,(4)-Tetrakis[(2-mercaptop)pyridine]phthalocyanine (I)	
2,3-Oktakis[(2-mercaptop)pyridine]phthalocyanine (II)	



Results and discussion

Polarization measurements

Figures 1a and 2 represents the potentiodynamic polarization curves of aluminum in 0.1 M HCl solutions in the absence and presence of various concentration of compounds **I** and **II**. It can be seen from figures, both of the anodic and cathodic current densities obtained in 0.1 M HCl solutions in the presence of phthalocyanines are lower than corrosion current densities obtained in acid solutions.

The electrochemical parameters such as corrosion potential (E_{corr}), corrosion current density (i_{corr}), cathodic Tafel slope (β_c), and anodic Tafel slope (β_a) obtained from polarization curves, and corresponding inhibition efficiency (η) values at different inhibitor concentrations are given in Table 2. Since the corrosion rate is directly related to the corrosion current density, the inhibition efficiency $\eta\%$ at different inhibitor concentrations were calculated from the following equation:

$$\eta\% = \frac{i_0 - i_1}{i_0} \times 100,$$

where i_0 and i_1 are the corrosion current densities in the absence and presence of the inhibitor, respectively.

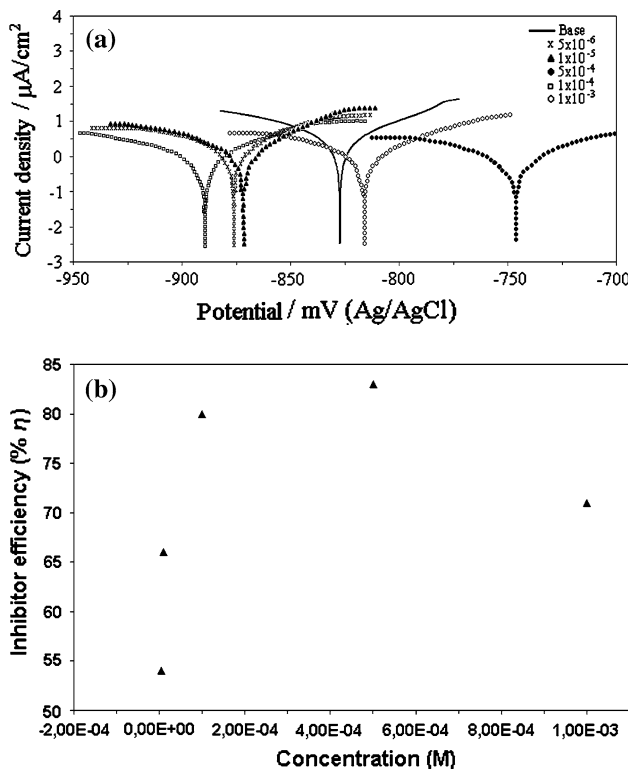


Fig. 1 a Potentiodynamic curves obtained for aluminum at 25 °C in 0.1 M HCl in the presence of phthalocyanines for compound **I**. b Inhibitor efficiency versus inhibitor concentration plot for compound **I** at 25 °C

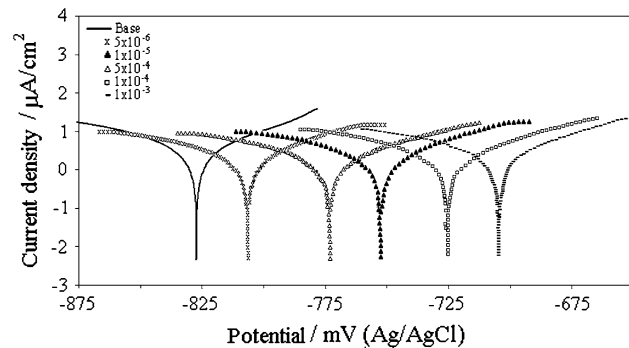


Fig. 2 Potentiodynamic curves obtained for aluminum at 25 °C in 0.1 M HCl in the presence of phthalocyanines for compound **II**

According to the Fig. 1b and the data of Table 2, it is seen that the inhibition efficiency increases with the inhibitor concentration increases and tends to attain a maximum value when the concentration reaches to 5×10^{-4} and 1×10^{-5} M for **I** and **II**, respectively. At these concentrations, maximum inhibition efficiency ($\eta\%$) is found to be 83% for compound **I** and 63% for compound **II**, respectively. Also the corrosion potential shift does not correlate with the inhibitor concentration at all. Figure 1a shows that there is a negative shift in potential for the 5×10^{-6} , 1×10^{-5} , and 1×10^{-4} but a positive shift (i.e., to more noble potentials) for 1×10^{-3} and 5×10^{-4} . These results can be explained with sandwich-type of phthalocyanines complex. Two- or three-dimensional structures can be formed by coordination of transition metals. As well-known macrocyclic compounds, they have highly delocalized large π -electron system that endows them many unique properties useful for many application [19–24]. Such extending of molecular structure brings various different behaviors of phthalocyanine. Our opinion is that phthalocyanines can be formed sandwich-type complex at higher concentration that

Table 2 Electrochemical parameters of corrosion of pure aluminum in the presence of different concentration of inhibitors at 25 °C and corresponding inhibition efficiencies from polarization method

Inhibitor	C (M)	E_{corr} (mV)	i_{corr} ($\mu\text{A}/\text{cm}^2$)	β_a (mV)	β_c (mV)	$\eta\%$
Base		-827.25	5.37	56.60	-96.30	-
I	5×10^{-6}	-875.80	2.45	53.20	-101.00	54
	1×10^{-5}	-871.90	1.78	47.40	-81.50	66
	1×10^{-4}	-816.10	1.59	62.20	-104.70	71
	5×10^{-4}	-889.30	1.08	55.60	-85.80	80
	5×10^{-3}	-746.10	0.92	61.50	-86.30	83
II	5×10^{-4}	-727.50	2.28	56.50	-66.70	58
	1×10^{-4}	-725.40	2.25	59.80	-78.30	58
	1×10^{-3}	-705.10	2.14	50.50	-68.30	60
	5×10^{-6}	-806.50	2.19	55.00	-82.40	59
	1×10^{-5}	-752.90	1.99	54.40	-66.80	63

is called critical concentration (CC). On complete inspection of Table 2, it can be observed that adsorption amount and the coverage of these inhibitors are saturated on the surface at low concentration. However, at the higher concentrations than CC, phthalocyanines form a complex with aluminum in the solution.

Electrochemical impedance measurement

Impedance spectra for aluminum in 0.1 M HCl, in the presence and the absence of various concentrations of phthalocyanines, were similar in shape. The appearance of two semicircles in the impedance diagram was common to all systems. The impedance diagrams show semi-circles indicating a barrier layer formed on the aluminum surface [5]. The semicircle radii were depending on the inhibitor used and its concentration. Nyquist plots for aluminum in HCl solution alone and in the presence of inhibitors are presented in Figs. 3 and 4.

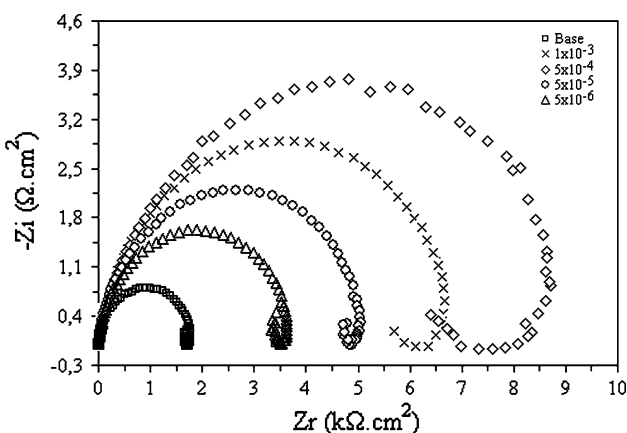


Fig. 3 Nyquist plots obtained at 25 °C in 0.1 M HCl in various concentrations for compound I

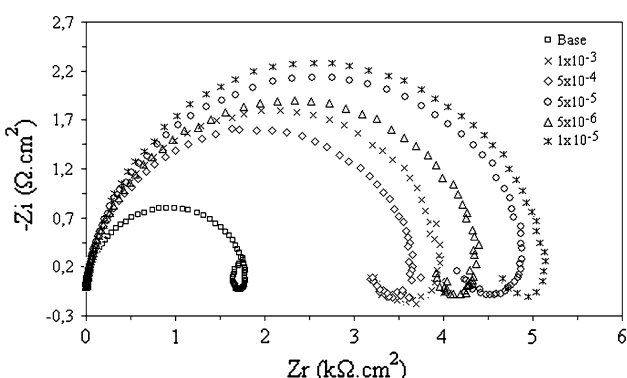


Fig. 4 Nyquist plots obtained at 25 °C in 0.1 M HCl in various concentration of compound II

Table 3 Impedance parameters and corresponding inhibition efficiency for the corrosion of aluminum in the 0.1 M HCl

Inhibitor	C_{inh} (M)	R_s (kΩ cm ²)	C_{dl} (μF/cm ²)	$\eta\%$
Base	—	1.81	13.82	
I	5×10^{-6}	3.76	17.87	51
	5×10^{-5}	5.19	17.17	64
	1×10^{-3}	7.02	14.32	74
	5×10^{-4}	9.17	17.96	80
	5×10^{-3}	3.75	11.88	52
II	1×10^{-3}	4.06	10.98	55
	5×10^{-6}	4.54	15.69	60
	5×10^{-5}	5.07	12.54	64
	1×10^{-5}	5.48	15.09	67

The effect of the inhibitors concentration on the impedance behavior of aluminum in 0.1 M HCl solution has been studied and the results are shown in Figs. 3 and 4. Inspections of the data reveal that, the impedance spectra consist of a large capacitive loop at high frequencies (HFs) followed by a small indicative one at low frequency (LF) range. In the investigated frequency range, similar impedance plots were reported for aluminum in HCl [3, 5, 24–28]. The HF capacitive loop is usually related to the charge transfer of the corrosion process and the inductive loop may be attributed to the relaxation processes in the oxide film covering electrode surface [25].

Values of R_s and C_{dl} at different inhibitor concentrations are given in Table 3. R_s and C_{dl} are the charge transfer resistance, double layer capacitance, respectively. The R_s values increase with the increasing in concentration of different phthalocyanines and tends to attain a maximum value when the concentration reaches to its critical concentration ($CC \sim 10^{-4}$ M at 25 °C), but decrease with an increase in temperature. On the other hand, the values of C_{dl} are almost the same for all concentrations. The inhibition efficiencies at different inhibitor concentrations were calculated using the following equation:

$$\eta\% = \frac{R_0 - R_1}{R_0} \times 100,$$

where R_0 and R_1 are the polarization resistance in the absence and presence of the inhibitor, respectively.

The equivalent circuit used to fit the experimental results is given in Fig. 5. The measured complex-plane impedance plot is similar to that calculated by the equivalent circuit model. It consists of a constant phase element (CPE) Q in parallel with series resistors R_1 and R_s , and an inductance, of magnitude L , in parallel with R_{ind} (Fig. 5).

The two different techniques (potentiodynamic polarization and EIS) gave the same trend of inhibition of the phthalocyanines and yield nearly the same values of $\eta\%$.

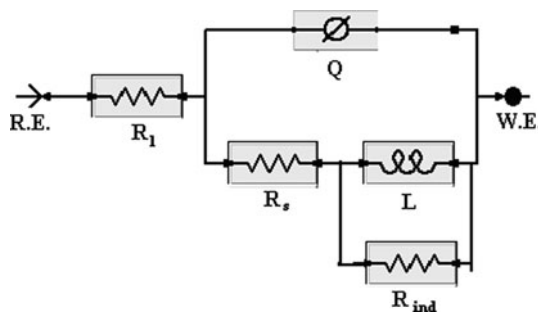


Fig. 5 The equivalent circuit model used to fit the experimental results

Adsorption isotherms

It has been assumed that organic inhibitors establish their inhibition via the adsorption of the inhibitor on to the metal surface. The inhibitor efficiency depends on the type and number of active sites at metal surface, the charge density, the molecular size of the inhibitor, the metal–inhibitor interaction, and the metallic complex formation [29–31].

Inhibition efficiencies of the investigated phthalocyanines increased as their concentrations were increased. This fact can be explained by the adsorption of these compounds on aluminum surface. Basic information on the interaction between the compounds and metal surfaces can be provided from the adsorption isotherms. The surface coverage values were calculated using the following equation:

$$\theta = \frac{R_1 - R_0}{R_1} = \frac{i_0 - i_1}{i_0},$$

where i_1 and i_0 are the corrosion current densities for with and without inhibitor, R_1 and R_0 are charge transfer resistance values with and without inhibitor, respectively. Therefore, several adsorption isotherms were tested for the description of adsorption behavior of studied compounds and it is found that adsorption of studied phthalocyanines on aluminum surface in HCl solution obeys the Langmuir adsorption isotherm given by following equations:

$$\frac{C_{\text{inh}}}{\theta} = \frac{1}{K_{\text{ads}} + C_{\text{inh}}},$$

where C_{inh} is the inhibitor concentration and K_{ads} is the adsorption equilibrium constant. The relation between C_{inh}/θ and C_{inh} at 25 °C is shown in Figs. 6 and 7. A linear relation can be found between C_{inh}/θ and C_{inh} . This behavior indicates that the adsorption of phthalocyanines on pure aluminum surface obeys Langmuir adsorption isotherm. This isotherm assumes that the adsorbed molecules occupy only one site, and there are no interactions with other molecules adsorbed.

The free energy of adsorption (G_{ads}) value of inhibitor molecule has been obtained by using following equation:

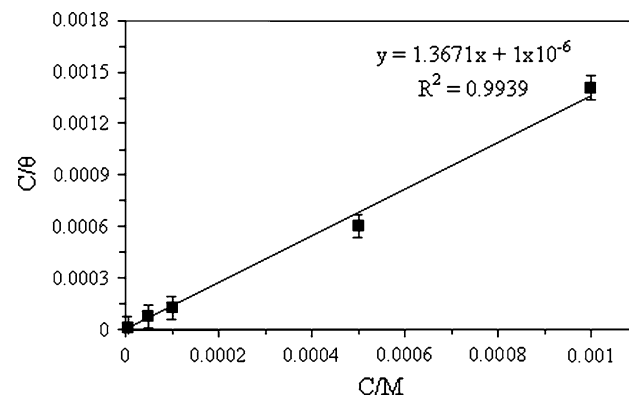


Fig. 6 Plot of Langmuir adsorption isotherm obtained by using surface coverage values calculated by polarization curves for compound I

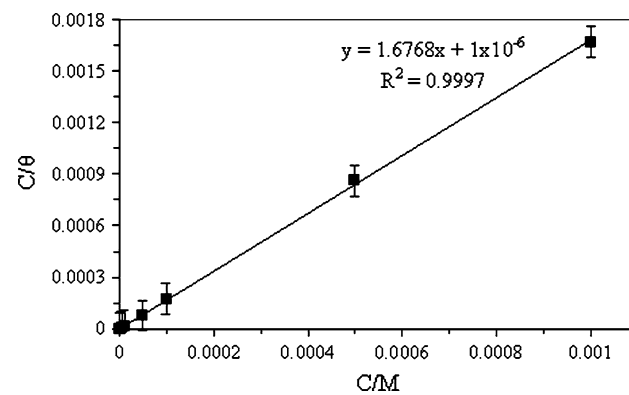


Fig. 7 Plot of Langmuir adsorption isotherm obtained by using surface coverage values calculated by polarization curves for compound II

$$K_{\text{ads}} = \frac{1}{55.5} \exp\left(\frac{-\Delta G_{\text{ads}}^{\circ}}{RT}\right).$$

The $\Delta G_{\text{ads}}^{\circ}$ value of adsorption process was calculated as –24.242 kJ/mol at the studied condition. The negative value of $\Delta G_{\text{ads}}^{\circ}$ indicates that the inhibitor is spontaneously adsorbed onto the aluminum surface. In the literature, negative values of $\Delta G_{\text{ads}}^{\circ}$ 20 kJ/mol or lower are attributed to the electrostatic interaction between the charged molecules and the charged metal (physisorption); those around 40 kJ/mol or higher involve charge sharing or transfer from organic molecules to the metal surface to form a coordinate type of bond (chemisorption) [25, 26]. The calculated value of $\Delta G_{\text{ads}}^{\circ}$ (–24.242 kJ/mol) shows that an electrostatic interaction between charged molecules and charged metal surface (physisorption) can occur [24]. Similar results were obtained from the data of the other technique (the figures are not presented here).

Effect of temperature

To find the activation energy of dissolution of aluminum, polarization measurements were performed at different temperatures (from 288 to 308 K) in the absence and presence of 5×10^{-4} M inhibitor **I**. The obtained curves are shown in Figs. 8 and 9. The calculated inhibition efficiency and other parameters are listed in Table 4.

Inhibition efficiency decreases considerably with the increases of temperature, confirming the suggestion that this inhibitor is physically adsorbed on the metal surface and the strength of the adsorption decreases with temperature.

The Langmuir adsorption isotherm may be expressed by following equation:

$$\log\left(\frac{\theta}{1-\theta}\right) = \log A + \log C - \frac{Q_{\text{ads}}}{2.303 \times R \times T}$$

where A is a constant and Q_{ads} is heat of adsorption and equal to enthalpy of adsorption (ΔH_{ads}) process [21]. Figure 10 represents the plot of $\log(\theta/1-\theta)$ versus $1/T$ for potentiodynamic measurements and impedance measurements. The heats of adsorption (Q_{ads}) are calculated from

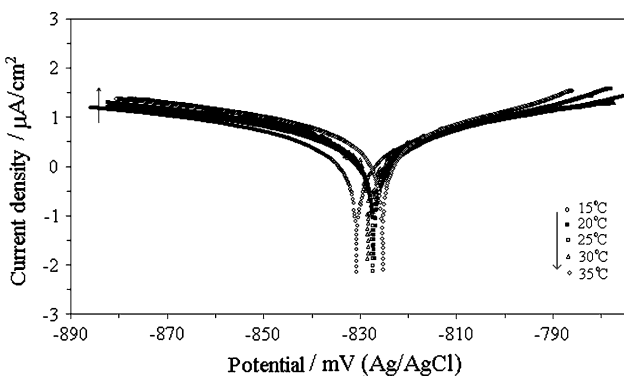


Fig. 8 Potentiodynamic curves of aluminum in the absence of compound **I** at different temperatures

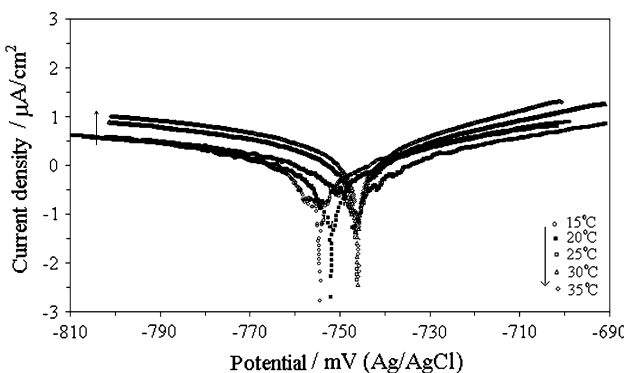


Fig. 9 Potentiodynamic curves of aluminum in the 5.0×10^{-4} M compound **II** at different temperatures

Table 4 Effect of solution temperature on kinetic parameters obtained from potentiodynamic polarization curves of aluminum in 0.1 HCl in the absence and presence of 5×10^{-4} M compound **I**

	Temperature (K)	E_{corr} (mV)	i_{corr} ($\mu\text{A}/\text{cm}^2$)	β_a (mV)	β_c (mV)	$\eta\%$
Base	288	-830.70	3.70	65.20	-85.10	
	293	-827.00	4.88	58.70	-104.10	
	298	-827.25	5.37	56.60	-96.30	
	303	-828.52	5.60	88.90	-77.60	
	308	-825.37	6.39	45.50	-94.50	
	I	-754.42	0.76	47.70	-64.20	85
I	293	-752.92	0.89	53.20	-78.20	83
	298	-746.25	0.92	61.50	-86.30	83
	303	-746.12	2.18	58.80	-100.10	59
	308	-745.82	2.75	50.80	-91.40	49

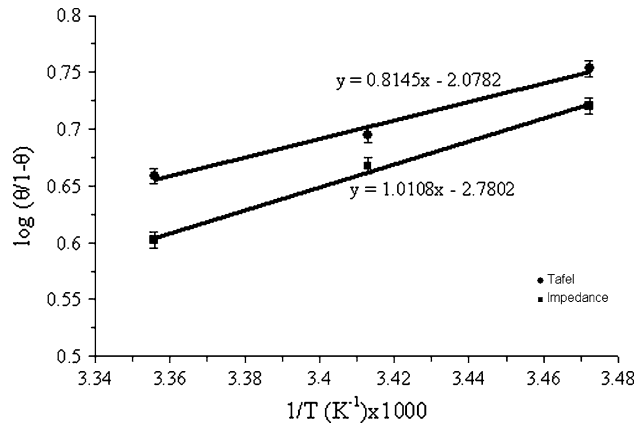


Fig. 10 Plot of Langmuir adsorption isotherm of compound **I** by using surface coverage values calculated by the EIS and Tafel results

the slopes of curves as -15.60 and -19.35 kJ/mol, respectively. The negative values of Q_{ads} indicated that the adsorption of used inhibitors on the aluminum surface is exothermic.

The entropy of adsorption process ($\Delta S_{\text{ads}}^\circ$) was obtained based on following thermodynamic basic equation:

$$\Delta G_{\text{ads}}^\circ = \Delta H_{\text{ads}}^\circ - T \cdot \Delta S_{\text{ads}}^\circ$$

The value of $\Delta S_{\text{ads}}^\circ$ was calculated as 42.69 J/(mol K). The positive value of $\Delta S_{\text{ads}}^\circ$ related to the increase of disorder results from the adsorption of the phthalocyanine molecule by desorption of more water molecules [32].

Conclusion

- It is seen that the inhibition efficiency increases when the inhibitor concentration increases and tends to attain a maximum value when the concentration reaches the

- critical concentration (CC). Phthalocyanines may be formed sandwich-type complex at CC.
2. Maximum inhibition efficiency ($\eta\%$) is found about 83% for quaternized 1,(4)-tetrakis[(2-mercaptopyridine]phthalocyanine (**I**). The two different techniques gave the same trend of inhibition of the phthalocyanines and yield nearly the same values of $\eta\%$.
 3. These compounds are acting as adsorption inhibitor so that the inhibition efficiency decreases with an increase in temperature. These suggest that physical adsorption may be type of adsorption. Adsorption of studied phthalocyanines on aluminum surface in HCl solution obeys the Langmuir adsorption isotherm. This isotherm assumes that the adsorbed molecules occupy only one site, and there are no interactions with other molecules adsorbed on the Al surface.

Acknowledgement Thanks to author Devrim Atilla and Mahmut Durmuş for synthesizing phthalocyanines. This project was supported by TÜBITAK (project no. MAG107M476).

References

1. Umoren S, Obot I, Obi-Egbedi N (2009) J Mater Sci 44:274. doi: [10.1007/s10853-008-3045-8](https://doi.org/10.1007/s10853-008-3045-8)
2. Aghion E, Lulu N (2009) J Mater Sci 44:4279. doi: [10.1007/s10853-009-3634-1](https://doi.org/10.1007/s10853-009-3634-1)
3. Metikos-Hukovic M, Babic R, Grubac Z (2002) J Appl Electrochem 32:35
4. Babic-Samardzija K, Hackerman N, Sovilj SP, Jovanovic VM (2008) J Solid State Electrochem
5. Yurt A, Ulutas S, Dal H (2006) Appl Surf Sci 253:919
6. Song M, Chen KH (2008) J Mater Sci 43:5265. doi: [10.1007/s10853-008-2573-6](https://doi.org/10.1007/s10853-008-2573-6)
7. Wang CY, Wu GH, Zhang Q et al (2008) J Mater Sci 43:3327. doi: [10.1007/s10853-008-2506-4](https://doi.org/10.1007/s10853-008-2506-4)
8. Xu WL, Yue TM, Man HC (2008) J Mater Sci 43:942. doi: [10.1007/s10853-007-2208-3](https://doi.org/10.1007/s10853-007-2208-3)
9. Pyun S, Moon S-M (2000) J Solid State Electrochem 4:267
10. Branzoi V, Golgovici F, Branzoi F (2002) Mater Chem Phys 78:122
11. Ashassi-Sorkhabi H, Shabani B, Aligholipour B, Seifzadeh D (2006) Appl Surf Sci 252:4039
12. Aoki IV, Guedes IC, Maranhao SLA (2002) J Appl Electrochem 32:915
13. Zhao P, Liang Q, Li Y (2005) Appl Surf Sci 252:1596
14. Agarwala VS (1984) Proc Int Cong Metal Corros 1:380
15. George RD, Snow AW (1995) J Heterocycl Chem 32:495
16. Young JG, Onyebeagu W (1990) J Org Chem 55:2155
17. Sehloho N, Durmuş M, Ahsen V, Nyokong T (2008) Inorg Chem Commun 11:479
18. Smith TD, Livorness J, Taylor HJ (1983) Chem Soc Dalton Trans 1391–1400
19. Sheldon RA (ed) (1994) Metalloporphyrins in catalytic oxidation. Dekker, New York
20. Duke SO, Reberz CA (eds) (1994) Porphyric pesticides—chemistry, toxicology, and pharmaceutical applications. American Chemical Society, Washington, DC
21. Tang CW (1986) Appl Phys Lett 48:183
22. Philip R, Ravikanth M, Kumar GR (1999) Opt Commun 165:91
23. Manas ES, Spano FC, Chen LX (1997) J Chem Phys 107(3):707
24. Abd el Rehim SS, Hassan HH, Amin MA (2001) Mater Chem Phys 70:64
25. Lee EJ, Pyun SI (1995) Corros Sci 37:157
26. Brett CMA (1992) Corros Sci 33:203
27. Brett CMA (1990) J Appl Electrochem 20:1000
28. Gojic M, Horvat R, Metikos-Hukovic M (1990) In: Proceedings of 6th European symposium corrosion inhibitors, vol 2, Ferrara, Italy, p 1099
29. Avci G (2008) Colloids Surf A Physicochem Eng Aspects 317:730
30. Donahue FM, Nobe K (1965) J Electrochem Soc 112:677
31. Khamis E, Bellucci F, Latanision RM, El-Ashry ESH (1991) Corrosion 47:677
32. Saleh MM (2006) Mater Chem Phys 98:83